Ab initio determination of electrical and thermal conductivity of liquid aluminum

Vanina Recoules*
Département de Physique Théorique et Appliquée, CEA/DAM Île-de-France, BP12, 91680 Bruyères-le-Châtel Cedex, France

Jean-Paul Crocombette
DEN/DMN/SRMP, CEA Saclay, 91191 Gif/Yvette, France
(Received 4 February 2005; published 8 September 2005)

We present here a technique to compute electronic thermal conductivity of fluids using quantum-molecular dynamics and the formulation of Chester-Tellung for the Kubo-Greenwood formula. In order to validate our implementation, the electrical and thermal conductivities of liquid aluminum were determined from 70 K above the melting point up to 10 000 K. Results agree well with experimental data for Al at 1000 K. The Lorentz number, defined as $K/\sigma T$, where K is the thermal conductivity, σ is the electrical conductivity, and T is the temperature, is close to the ideal value of 2.44×10^{-8} for metals, and the Wiedemann-Franz law is verified.

DOI: 10.1103/PhysRevB.72.104202 PACS number(s): 65.20.+w, 72.15.Cz

I. INTRODUCTION

Transport coefficients are commonly used to characterize the state of plasma. From the theoretical point of view, there are many models that predict the electrical and thermal conductivity, using various assumptions about electronic and ionic structure.[1–4] In the partially degenerate strongly coupled regime, those quantities are difficult to obtain because ion-ion interaction is screened by the electronic polarization, and there has been no correct model to account for nonlinear screening. Quantum-molecular dynamics (QMD) is ideally suited for this type of problem, precisely because no adjustable parameters or empirical interionic potentials are needed. Quantum determination of electrical conductivity using Kubo-Greenwood in the framework of density functional theory has been successfully used on various systems such as liquid and dense plasmas.[5–9]

The Lorentz number L is defined as

$$L=\frac{K}{\sigma T}=\gamma\frac{e^2}{k^2}, \tag{1}$$

where T is the temperature, K is the thermal conductivity, and σ is the electrical conductivity. γ depends on the law of forces responsible for the scattering of the electrons.[10] In the degenerate regime (liquids), γ is $\pi^2/3$ and L is 2.44×10^{-8}. This is the Wiedemann-Franz law. For the nondegenerate case (completely ionized gas), γ is 1.5966 (L is 1.18×10^{-8}).[11] In the intermediate region, there is no assumption on the γ value, and one cannot use the Wiedemann-Franz law to deduce thermal conductivity from the electrical conductivity. A theory that gives directly thermal conductivity is then highly interesting.

In this paper, we present a direct evaluation of thermal conductivity using quantum-molecular dynamics based on plane-wave density functional theory and the Kubo-Greenwood formula in the Chester-Tellung version.[10] This technique has been used to model the electronic transport properties of quasicrystals[12] and of disordered solids[13] using the atomic-sphere approximation of the linear muffin-tin orbitals (ASA-LMTO) method. In order to validate our implementation of quantum computation of thermal conductivity, we have calculated the electronic transport property of liquid aluminum near the melting point. Indeed, several experimental and theoretical data are available near this particular point. Then, we present a calculation of electrical and thermal conductivity of modeled liquid aluminum at temperature up to $T=10\,000$ K with a fixed ionic density of 2.35 g/cc, which is the experimental liquid density near the melting point. In this regime, the γ parameter is expected to be $\pi^2/3$.

This paper is organized as follows: In the next section, we will describe the quantum simulations and Kubo-Greenwood formulation of Chester-Tellung for electrical and thermal conductivity. In Sec. III, our results for aluminum at $T=1000$ K are checked against experimental results. Finally, the evolution of electrical and thermal conductivity vs temperature are discussed.

II. THEORETICAL METHOD

QMD simulations for liquid Al were performed at several temperatures ranging from $T=1000$ K to $T=10\,000$ K, at experimentally measured liquid density. 108 particles were treated in a cubic cell of the size appropriate to the experimental density of 2.35 g/cc. First, ionic structures are generated with the VASP (Vienna *ab initio* Simulation Program) plane-wave code developed at the Technical University of Vienna,[14] in the framework of a finite temperature-density functional theory. Ion-electron interactions are described with the projected augmented wave (PAW) method given by Kresse *et al.* [15,16] The Perdew and Wang parametrization of the generalized gradient approximation[17] is used for the exchange and correlation potential. After thermalization, each temperature point was simulated for about 1 ps in the microcanonical ensemble. Electronics levels are occupied according to Fermi-Dirac statistics, with electronic temperature set equal to that of ions. We consider electronic states occupied down to 10^{-6}. The QMD calculations are performed using only the Γ point for representation of the Brillouin zone, with

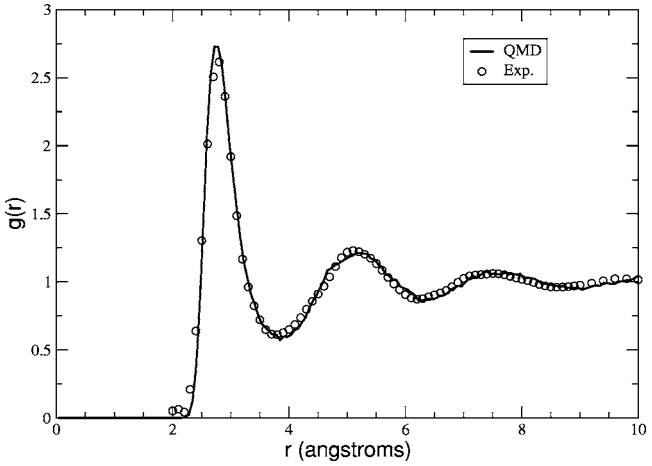

FIG. 1. Calculated radial distribution function for liquid Al at $T=1000$ K (solid line) compared with experimental data (Ref. 27) (open circles).

a plane-wave cutoff of 300 eV. The Γ-point sampling is expected to be a good approximation for calculating the structure and dynamics of liquid aluminum, but is not enough for accurate calculation of electronic properties such as electrical or thermal conductivity.

For selected statistically independent atomic configurations, a self-consistent ground-state calculation is performed with the ABINIT code[18] to get the detailed electronic structure. The electronic calculation is done in the generalized gradient approximation with the exchange-correlation energy functional of Perdew-Burke-Ernzerhof.[19] Orbitals are expanded in plane waves up to a cutoff of 165 eV. A $2\times2\times2$ Monkhorst-Pack **k**-points mesh is used in the Monkhorst-Pack scheme. The total energy convergence has been checked against the plane-wave cutoff energy and number of **k** points to obtain a convergence up to 0.1 meV. The pseudopotential used in our work is generated by the Troullier-Martins method[20]—$3s$ and $3p$ states are treated as valence electrons, and we use a d nonlocal part.

The linear response of a system to an electrical field **E** and temperature gradient ∇T is characterized by the electrical and heat current densities, respectively j and j_q. These two quantities are related to the electric field **E** and to the temperature gradient ∇T by (Onsager relations)

$$\langle j\rangle = \frac{1}{e}\left(e\mathcal{L}_{11}\mathbf{E} - \frac{\mathcal{L}_{12}\nabla T}{T}\right), \tag{2}$$

and

$$\langle j_q\rangle = \frac{1}{e^2}\left(e\mathcal{L}_{21}\mathbf{E} - \frac{\mathcal{L}_{22}\nabla T}{T}\right), \tag{3}$$

where e is the electron charge. The kinetic coefficients $\mathcal{L}_{ij}$ are the key to calculate electronic transport properties theoretically. Using Ohm's law, one obtains the electrical conductivity σ

$$\sigma = \mathcal{L}_{11}. \tag{4}$$

Electronic thermal conductivity K is

$$K = \frac{1}{eT}\left(\mathcal{L}_{22} - \frac{\mathcal{L}_{12}^2}{\mathcal{L}_{22}}\right). \tag{5}$$

In the Chester-Tellung-Kubo-Greenwood formulation, the kinetic coefficients $\mathcal{L}_{ij}$ are given by

$$\mathcal{L}_{ij} = (-1)^{(i+j)}\int d\epsilon\hat{\sigma}(\epsilon)(\epsilon-\mu)^{(i+j-2)}\left(-\frac{\partial f(\epsilon)}{\partial\epsilon}\right), \tag{6}$$

where $f(\epsilon)$ is the Fermi-Dirac distribution function, and μ is the chemical potential. $\hat{\sigma}(\epsilon)$ is calculated by means of the Kubo-Greenwood formula (Refs. 21 and 22)

$$\hat{\sigma}(\epsilon) = \frac{he^2}{\Omega}\sum_{k,k'}\langle\psi_k|\hat{\mathbf{v}}|\psi_{k'}\rangle\langle\psi_{k'}|\hat{\mathbf{v}}|\psi_k\rangle\delta(\epsilon_k-\epsilon_{k'}-\epsilon), \tag{7}$$

where Ω is the volume of the cell simulation, ϵ_k are the electronic eigenvalues, and $\langle\psi_k|\hat{\mathbf{v}}|\psi_{k'}\rangle$ are the velocity matrix elements.

By using the properties of the Dirac functions, Eq. (6) can be rewritten as

$$\mathcal{L}_{ij} = (-1)^{(i+j)}\frac{he^2}{\Omega}\lim_{\epsilon\to0}\frac{f(\epsilon_k')-f(\epsilon_k)}{\epsilon}\delta(\epsilon_k'-\epsilon_k-\epsilon) \times\sum_{k',k}\langle\psi_k|\hat{\mathbf{v}}|\psi_k'\rangle\langle\psi_{k'}|\hat{\mathbf{v}}|\psi_k\rangle(\epsilon_k'-\mu)^{i-1}(\epsilon_k-\mu)^{j-1}. \tag{8}$$

Equations (4) and (5) are applied to the energy-dependent form of the kinetic coefficient. Then, by extrapolating to zero energy, the electrical and thermal conductivities are obtained.

As the Troullier-Martins potential is nonlocal, we cannot use the momentum operator to represent the velocity operator, as is done elsewhere. We use the definition of the velocity operator

$$\hat{\boldsymbol{v}} = \frac{i}{\hbar}[\hat{H},\boldsymbol{r}]. \tag{9}$$

$\hat{H}$ represents the total Hamiltonian of the system. Then, $\hat{\mathbf{v}}$ is expressed in terms of $\partial\hat{H}/\partial\boldsymbol{k}$. Technical details on the computation of matrix elements can be found in Refs. 23 and 24.

The chemical potential is obtained by fitting the set of occupation numbers corresponding to the set of eigenvalues with the usual functional form for the Fermi-Dirac distribution at finite temperature. The δ function must be broadened—it is replaced by a Gaussian function. The Gaussian broadening is tested to obtained smooth and well-converged curves.

III. RESULTS

A. Aluminum at $T=1000$ K

To support the quality of the QMD simulation, the calculated radial-distribution function is shown in Fig. 1, compared with experimental data measured by x-ray diffraction experiments. Radial-distribution functions were averaged during all the simulations. The present result agrees with the experimental data. The level of agreement between experiment and theory is comparable to that obtained in previous

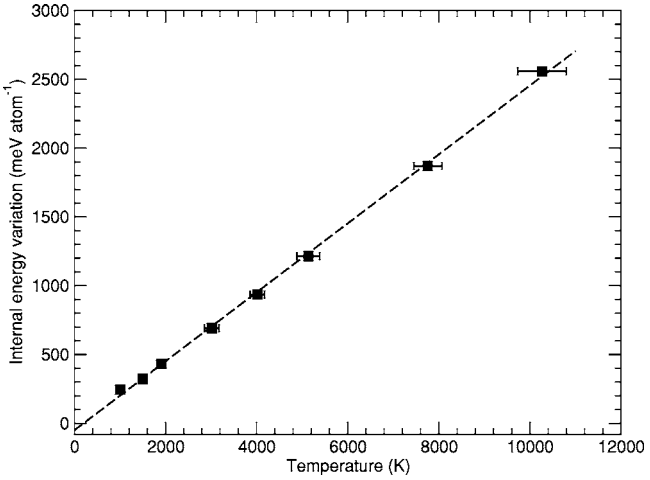

FIG. 2. Internal energy variation (solid squares) vs temperature. The dashed line is a linear fit of data.

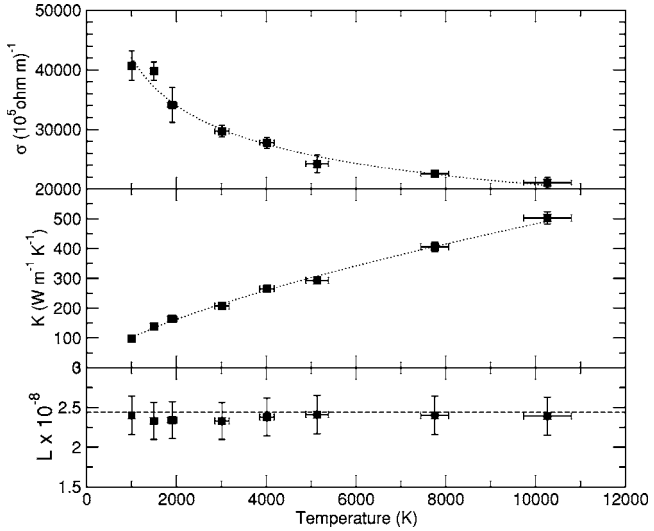

FIG. 3. Electrical conductivity, thermal conductivity, and Lorentz number as a function of temperature. The dashed line is for readability. For the Lorentz number, the dashed line is the value of the degenerate limit.

quantum-molecular-dynamics studies.[25,26] We verified that the mean-square displacement increases during the simulation, which is characteristic of a liquid state.

Once the ionic-liquid structure is correct, optical conductivity $\sigma(\omega)$ vs frequency ω is computed by averaging over optical conductivities from six snapshots selected during the course of QMD simulation. The extrapolation to zero frequency must be performed carefully, since in a finite system, energy levels are always discrete and $\sigma(\omega)$ falls to zero for small values of ω (Ref. 5). Therefore, it is more convenient to use a functional form for extrapolating to zero. In metallic aluminum, conductivity is carried by free electrons. It has been shown that a natural functional form for fitting the calculated $\sigma(\omega)$ in this regime is the Drude formula (Ref. 7)

$$\sigma(\omega) = \frac{\sigma}{1 + \omega^2 \tau^2}, \tag{10}$$

where τ is the relaxation time. Using this fit, the zero-frequency limit yields the dc conductivity. The value obtained, $\sigma_{\mathrm{dc}} = 40.7 \times 10^5\ \Omega\ \mathrm{m}^{-1}$, is close to the experimental value, $39.7 \times 10^5\ \Omega\ \mathrm{m}^{-1}$, and close to the value obtained with a similar technique by Alemany *et al.*[25]

For the same six snapshots, Eq. (5) is computed, leading to a frequency-dependent expression. Thermal conductivity is evaluated by extrapolating to zero frequency. The value obtained for thermal conductivity $K = 98\ \mathrm{W\ m^{-1}\ K^{-1}}$ is in the range of the experimental values [between 95 and 98 $\mathrm{W\ m^{-1}\ K^{-1}}$ (Ref. 28) and references therein].

Using the preceding experimental values, the Lorentz ratio is between 2.40×10^{-8} and 2.46×10^{-8}. For liquid aluminum at $T = 1000$ K, the computed Lorentz number is 2.41×10^{-8}, which is very close to the ideal value of Lorentz number predicted by the nearly free electron model. This model is applicable in cases where scattering of the electrons by the ions is sufficiently weak to justify the Born approximation, which is true of simple metals such as aluminum.

B. Temperature-dependent results

Electrical and thermal conductivity are computed for eight-temperatures ranging from $T = 1000$ K to $T = 10\,000$ K. The volume is kept constant so that there is no vaporization and the system remains liquid even at $T = 10\,000$ K.

From QMD trajectory, the internal energy is extracted. Figure 2 presents the internal energy for various temperatures. Internal energy variation is linear in T. Using a linear fit, one can deduce the heat capacity for liquid aluminum. The value obtained is $C_v = 25.3 \pm 2.0\ \mathrm{J\ mol^{-1}\ K^{-1}}$, which is in accordance with the literature value $C_v = 29\ \mathrm{J\ mol^{-1}\ K^{-1}}$ (Ref. 29).

The electrical conductivity, thermal conductivity, and Lorentz number as a function of temperature are plotted in Fig. 3.

As expected for a liquid metal, electrical conductivity decreases with temperature, whereas thermal conductivity increases. In metals, one can perform the approximation so that the first term in Eq. (5) exceeds the second term by a factor of order $(\epsilon_f / k_B T)^2$, where ϵ_f is the Fermi energy. Thus,

$$K = \mathcal{L}_{22}. \tag{11}$$

We verify that this is true for all temperatures. The fact that $K = \mathcal{L}_{22}$ in all the domains explored shows the validity of the technique employed here. For all temperatures, we obtained a Lorentz number slightly below the ideal value. The calculated Lorentz numbers are between 2.40 and 2.30 for the different temperatures. At those temperatures, the Lorentz number might be constant and equal to the limit value for the degenerate case. We showed that the Lorentz number is still close to the ideal value for metals.

IV. CONCLUSION

In conclusion, we have demonstrated the feasibility of calculating thermal conductivity from quantum-molecular dynamics using the Kubo-Greenwood formula in the formulation of Chester-Tellung. For liquid aluminum, 70 K above the fusion point, the computed electrical resistivity and thermal conductivity agree well with experimental data. When the temperature increases up to $T = 10\,000$ K, the Lorentz number is still close to the limit 2.44×10^{-8} for the degenerate system for all the temperature domains explored. The technique employed is also applicable for strongly coupled plasma.

ACKNOWLEDGMENTS

We gratefully acknowledge S. Bernard for supplying the pseudopotential and J. Clérouin, P. Renaudin, and A. Decoster for useful discussions.

*Electronic address: vanina.recoules@cea.fr

[1] L. Spitzer and R. Harm, Phys. Rev. **89**, 977 (1953).
[2] Y. T. Lee and R. M. More, Phys. Fluids **27**, 1273 (1983).
[3] G. A. Rinker, Phys. Rev. A **37**, 1284 (1988).
[4] H. Kitamura and S. Ichimaru, Phys. Rev. E **51**, 6004 (1995).
[5] P. L. Silvestrelli, Phys. Rev. B **60**, 16382 (1999).
[6] M. P. Desjarlais, J. D. Kress, and L. A. Collins, Phys. Rev. E **66**, 025401(R) (2002).
[7] V. Recoules, P. Renaudin, J. Clérouin, P. Noiret, and G. Zérah, Phys. Rev. E **66**, 056412 (2002).
[8] V. Recoules, J. Clérouin, P. Renaudin, P. Noiret, and G. Zérah, J. Phys. A **36**, 1 (2002).
[9] J. Clérouin, Y. Renaudin, P. Laudernet, P. Noiret, and M. P. Desjarlais, Phys. Rev. B **71**, 064203 (2005).
[10] G. V. Chester and A. Thellung, Proc. Phys. Soc. London **77**, 1005 (1961).
[11] H. Reinholz, R. Redmer, and S. Nagel, Phys. Rev. E **52**, 5368 (1995).
[12] C. V. Landauro and H. Solbrig, Phys. Fluids **27**, 1273 (1983).
[13] C. Villagonzalo, R. A. Römer, and M. Schreiber, Eur. Phys. J. B **12**, 179 (1999).
[14] G. Kresse and J. Hafner, Phys. Rev. B **47**, R558 (1993).
[15] G. Kresse and D. Joubert, Phys. Rev. B **59**, 1758 (1999).
[16] P. E. Blöchl, Phys. Rev. B **50**, 17953 (1994).
[17] J. P. Perdew, *Electronic Structure of Solids* (Akademie Verlag, Berlin, 1991).
[18] X. Gonze, J.-M. Beuken, R. Caracas, F. Dutraux, M. Fuchs, G.-M. Rignanese, L. Sindic, M. Verstraete, G. Zerah, F. Jollet *et al.*, Comput. Mater. Sci. **25**, 478 (2002).
[19] J. P. Perdew, K. Burke, and M. Ernzerhof, Phys. Rev. Lett. **77**, 3865 (1996).
[20] N. Troullier and J. L. Martins, Phys. Rev. B **43**, 1993 (1991).
[21] R. Kubo, J. Phys. Soc. Jpn. **12**, 570 (1957).
[22] D. A. Greenwood, Proc. Phys. Soc. London **71**, 585 (1958).
[23] X. Gonze, Phys. Rev. B **55**, 10337 (1997).
[24] X. Gonze and C. Lee, Phys. Rev. B **55**, 10355 (1997).
[25] M. M. G. Alemany, L. J. Gallege, and D. J. Gonzàlez, Phys. Rev. B **70**, 134206 (2004).
[26] L. Vocadlo and D. Alfe, Phys. Rev. B **65**, 214105 (2002).
[27] Y. Waseda, *The Structure of Non-Crystalline Materials* (Mc Graw-Hill, New York, 1980).
[28] W.-K. Rhim and T. Ishikama, Rev. Sci. Instrum. **69**, 3628 (1998).
[29] G. R. Gathers, Int. J. Thermophys. **4**, 209 (1983).